OPEN

A Hypothesis Generating the Mechanical Systems Underlying Posterior Vaginal Prolapse Based on Observed Displacements by Dynamic Magnetic Resonance Imaging

Zhongyuan Qiu, MD and Yanfeng Song, PhD

Objective: The aim of this study was to analyze quantified displacements of the posterior vaginal wall (PVW) on dynamic magnetic resonance imaging (MRI), which may generate hypotheses for the detailed mechanisms that underlie the development of posterior vaginal prolapse.

Methods: Pelvic dynamic MRI scans were obtained for 12 women with normal vaginal structure (stage 0) and 62 women with 4 consecutive stages (1–4) of posterior vaginal prolapse. Structural locations (apex vagina, distal vagina, and mid–perineal body [PB]) and equidistant points along the PVW (points 4–6 were considered as midvagina) were identified, and PVW length, straight distance of PVW, levator ani parameters (levator hiatus length [LHL], levator hiatus width [LHW], levator plate angle, anorectal angle, and M line [ML]), urogenital hiatus, and prolapse diameter were measured at rest and maximal Valsalva, respectively. The displacement of these measurements was obtained.

Results: From stage 0 to 2, the variables LHL, LHW, levator plate angle, anorectal angle, and ML increased gradually, but midvagina, distal vagina, and mid-PB were the opposite. From stage 2 to 3, apex vagina, midvagina, distal vaginal, mid-PB, LHL, LHW, and ML raised rapidly and peaked at stage 3, then declined at stage 4. In addition, the correlation coefficients between each measurement from stage 2 to 3 were statistically higher than those from stage 0 to 2.

Conclusions: Quantified displacements of the PVW and its supporting structure were shown on dynamic MRI, and the mechanical mechanisms were hypothesized regarding the interaction between pressure and the support force contributing to the deformation of the PVW and the supporting structures.

Key Words: dynamic magnetic resonance imaging, hypothesis, mechanical mechanism, posterior vaginal prolapse, support structure

(*Female Pelvic Med Reconstr Surg* 2020;26: 585–590)

Statistics show that each year more than 200,000 operations are performed to repair vaginal prolapse in the United States alone.[1] Repair of posterior vaginal prolapse (PVP) was consisted in 87% of all pelvic surgeries,[2] and literature indicates that 25% to 29% of patients will require a second surgical intervention.[3,4] However, posterior pelvic floor problems were actually neglected in urogynecology.[5] Although the reason of impairment of pelvic floor is considered universally, the interaction of the pressure and the support force results in the deformation of posterior vagina wall and the supporting structures as the PVP progression has not been described; thus, the underlying mechanism of PVP remains unclear.

At present, dynamic magnetic resonance imaging (MRI) has established as a multiplanar global evaluation method for assessing pelvic contents, and the treatment of pelvic floor dysfunction is increasingly dependent on preoperative imaging.[6] Existing MRI has indicated that the relative locations of the perineal structures and the apex vagina are more caudally positioned in the posterior vaginal wall (PVW) than in normal conditions at maximal Valsalva state.[7] Besides, there are clear differences in movement along the length of the anterior and PVW when compared between a resting state and maximum Valsalva.[8] However, static images do not provide information regarding the conduction of pressure in the pelvic region, and there are no possible methods to test and verify at present.

In this study, we conducted a detailed analysis of the physical displacement of pelvic floor structures in patients with progressive degrees of PVP as measured via dynamic MRI. Based on observed displacements of portions of the PVW under Valsalva loading, we have made several inferences regarding possible mechanisms that underlie the development of PVP. We believe that observing the correlation between displacement of one structure relative to another may provide insight regarding how the interaction between pressure and supporting force causes the deformation of PVW and the supporting structures as prolapse progresses.

MATERIALS AND METHODS

Sixty-two women with rectocele-type PVP and 12 volunteers with normal vaginal support were selected from the urogynecology clinic of the Fuzhou General Hospital, Fuzhou, Fujian Province, China. All patients with PVP had the PVW extended lower than the most dependent part of the anterior wall or cervix. All subjects received gynecology examinations, completed the Pelvic Organ Prolapse Quantification System (POP-Q), and underwent dynamic MRI. According to POP-Q staging, women with PVP were divided into 4 groups: stages 1, 2, 3, and 4, and women defined as stage 0 were healthy, nulliparous volunteers without PVP. Women who had histories of previous hysterectomy or other surgeries for pelvic floor disorders were excluded. Ethical approval was provided by the hospital's ethics committee, and informed consent was obtained from all participants.

With subjects in the supine position, MRI of the pelvic cavity was performed using a Siemens Magnet Trio 3.0 T System (Siemens, Munich, Germany). Three-dimensional (3D)-T2 sequences were used to obtain resting-state MRI scans in the sagittal, coronal, and axial planes. The parameters used for 3D-T2 sequencing were as follows: repetition time = 1600 milliseconds, time to echo = 97 milliseconds, field of view = 400 cm, and slice thickness 1.0 mm, interleaved with no gap. Subjects were instructed to carry out a maximal Valsalva maneuver for approximately 15 seconds in order to acquire images of PVW protrusion using a fast-spin proton density technique. Each subject was scanning at least 3 times repeatedly, and it was ensured that the maximal extent of prolapse seen during clinical examination was

From the Department of Obstetrics and Gynecology, Fuzong Clinical College of Fujian Medical University, Fuzhou, China.

Correspondence: Yanfeng Song, PhD, Department of Obstetrics and Gynecology, Fuzong Clinical College of Fujian Medical University, 156 West Second Ring North Road, Fuzhou, Fujian 350025, China.
E-mail: songyanfeng120@163.com.

The authors have declared they have no conflicts of interest.

DOI: 10.1097/SPV.0000000000000637

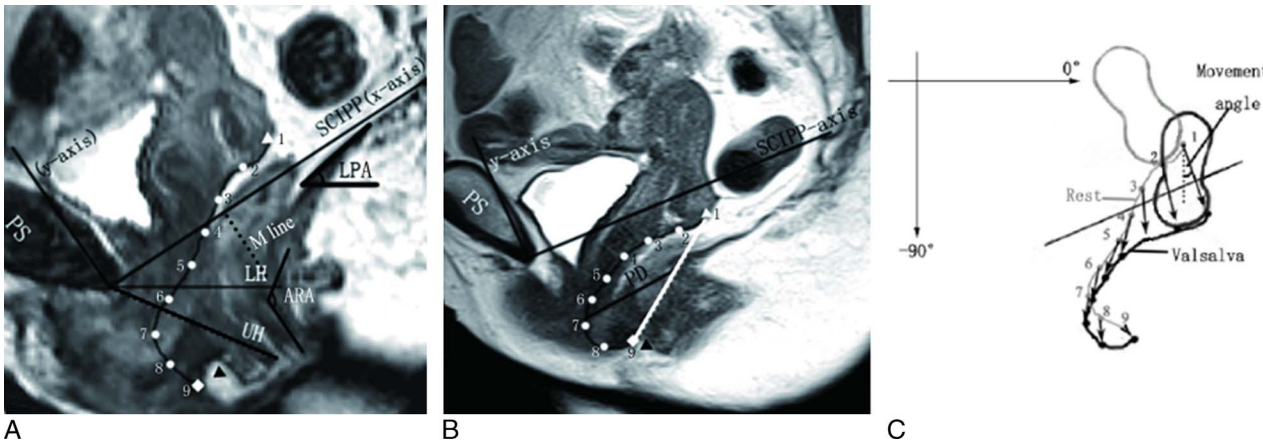

FIGURE 1. Magnetic resonance imaging of a PVP in a state of rest (A) and at maximum Valsalva (B). A, Sacrococcygeal-inferior pubic point (SCIPP) line and pubic symphysis (PS) along with mid-PB (black triangle), apex vagina (white triangle), distal vagina (white diamond), and 7 remaining locations (round white dots) along the PVW. The ML (black dotted line) is drawn perpendicularly from the posterior wall of the anorectal junction to the SCIPP line. The levator hiatus (LH), levator plate (LP), and UH are also labeled (black lines). B, Demarcation of the maximum PD and straight-line distance (white line) from the apex vagina to the distal vagina. C, Derivation of the displacement direction for the PVP.

reproduced in the scanner. General structural identifications were analyzed by the same radiologist and urogynecologist, who were blinded to the clinical status of the examined patient.

Using the analogical method in previous reports,[7,8] 9 locations with numbers 1 through 9 equidistantly for PVW and mid–perineal body (PB) were designated (locations 4–6 were considered midvagina); the straight-line distance of PVW (between apex vagina and distal vagina), PVW length, urogenital hiatus (UH), and levator ani (LA) diameters (levator hiatus length [LHL], levator plate angle [LPA], anorectal angle [ARA], and M line [ML]) were determined. We also calculated the parametric estimation between the most anterior point of the puborectalis and the most ventral point of the PVW, which thus determined the widest anterior-posterior prolapse diameter (PD).[7] Besides, we used transverse sections to record the levator hiatus width (LHW) at the bottom of pubic symphysis. A sacrococcygeal-inferior pubic point line (*x* axis) and perpendicular line (*y* axis)[9,10] were used to align images to correct the different pelvic inclinations in different examination positions during MRI scanning from rest to maximum Valsalva. The displacement vectors of corresponding landmarks were then calculated for each subject, and the mean displacements of locations 4 to 6 were considered as the movement value for the midvagina. The variation of movement angle of each location between the direction of movement and the long axis of the body was also measured from the resting state to maximum Valsalva (Fig. 1).

Data are exhibited as means ± SD and were tested for normality using the Kolmogorov-Smirnov test. Continuous variables were analyzed using analysis of variance (ANOVA) combined with a post hoc multiple-comparisons test. Correlation analysis was performed by determining Spearman correlation coefficients. $P = 0.05$ was regarded as the level of statistical significance. All data were analyzed with SPSS software IBM SPSS Statistics 21 (SPSS Inc, Chicago, Ill).

RESULTS

Demographic data for all subjects are shown in Table 1. Among the study participants, there were no significant differences in age, weight, body mass index, vaginal parity, history of forceps midwifery, and postmenopause. Statistically significant differences were found among the 5 groups in terms of point D and point Bp on the clinical POP-Q physical examination.

The mean measured displacement values of each group for PVW support systems from resting state to maximum Valsalva are shown in Table 2. Landmarks of vaginal support (level I represents apex vagina; level II, midvagina; level III, distal vagina and mid-PB[11]), LHL, LHW, ML, UH, and 1 to 9 locations along the

TABLE 1. Clinical Characteristics of the Different Patient Cohorts Investigated

Characteristics	Stage 0 (n = 12)	Stage 1 (n = 18)	Stage 2 (n = 24)	Stage 3 (n = 11)	Stage 4 (n = 9)	ANOVA *P*
Age, y	64.3 ± 8.4	61.7 ± 15.3	64.6 ± 10.3	60.0 ± 14.5	71.2 ± 9.6	0.270
Weight, kg	56.3 ± 9.2	56.3 ± 6.4	60.2 ± 7.4	67.2 ± 10.3	54.9 ± 7.2	0.324
BMI, kg/m^2	22.6 ± 3.4	22.4 ± 2.2	23.9 ± 2.0	23.0 ± 3.3	22.2 ± 2.3	0.078
Vaginal parity	3.8 ± 0.9	3.0 ± 1.2	2.9 ± 1.3	3.1 ± 1.4	3.9 ± 1.9	0.092
Rate of forceps midwifery, %	0	5.6	16.7	45.5	55.6	0.01
Post-menopause, %	83.3	77.8	75.0	72.7	100.0	0.107
D point, cm	−8.5 ± 1.2	−6.7 ± 1.9	−6.5 ± 1.9	−4.5 ± 3.2	−0.9 ± 3.8	0.001
Bp point, cm	−2.8 ± 0.4	−1.9 ± 0.3	0.3 ± 0.8	1.7 ± 1.3	4.4 ± 0.7	0.001

Values are reported as either percent (where indicated) or mean ± SD.
BMI indicates body mass index.

TABLE 2. Variation of Various Clinical Parameters Related to Vaginal Prolapse

Landmark	Stage 0 (n = 12)	Stage 1 (n = 18)	Stage 2 (n = 24)	Stage 3 (n = 11)	Stage 4 (n = 9)
Apex vagina, mm	25.33 ± 16.98	27.21 ± 13.17	30.93 ± 16.85	42.65 ± 16.80	30.33 ± 15.62
Midvagina, mm	18.34 ± 10.20	16.30 ± 8.48	15.61 ± 10.10	24.95 ± 13.91	19.93 ± 9.83
Distal vagina, mm	15.00 ± 8.98	13.46 ± 9.07	12.16 ± 8.82	22.73 ± 14.16	11.76 ± 3.38
Mid-PB, mm	26.19 ± 7.80	23.47 ± 9.47	22.17 ± 8.82	36.96 ± 10.54	30.01 ± 5.60
LHL, mm	5.30 ± 3.89	7.18 ± 3.11	9.43 ± 6.23	12.47 ± 7.14	7.17 ± 4.68
LHW, mm	3.79 ± 2.39	3.89 ± 3.26	9.51 ± 7.22	13.48 ± 9.56	6.40 ± 9.73
ML, mm	3.98 ± 3.87	5.49 ± 5.12	6.39 ± 5.18	12.66 ± 9.78	6.83 ± 6.61
LPA, °	9.48 ± 3.93	10.68 ± 6.24	10.95 ± 7.06	16.76 ± 5.72	18.20 ± 7.95
ARA, °	8.76 ± 4.47	9.04 ± 5.44	12.52 ± 5.72	14.00 ± 8.85	16.99 ± 10.12
PVW length, mm	−8.01 ± 11.20	6.97 ± 17.30	−0.36 ± 22.62	14.24 ± 26.49	36.41 ± 20.40
Straight distance of PVW, mm	−3.87 ± 8.81	−7.21 ± 5.81	−8.27 ± 6.10	−5.41 ± 7.40	−3.74 ± 11.76
UH, mm	5.13 ± 6.07	5.47 ± 3.34	5.04 ± 4.65	7.92 ± 6.29	2.63 ± 3.66
Prolapse diameter, mm	30.07 ± 9.95	36.01 ± 7.87	37.20 ± 9.22	46.09 ± 10.32	57.89 ± 10.53

Values are reported as mean ± SD.

Midvagina indicates mean displacement of points 4 to 6.

PVW exhibited higher displacement in stage 3 than other stages, and the variation of LPA and ARA climbed as the stage increased (Figs. 2 and 3A).

In addition, the entire PVW shifted downward; the movement angle for the upper and lower portions of PVW was posterior toward the rectum and slightly caudal, whereas the middle portions of PVW moved ventral. The vaginal wall displacement direction differed among the 5 groups (Fig. 3B). The result of the movement angle is shown in Table 3, and movement angles of wall locations 5 to 8 were significantly different between stages 3 to 4 and stages 0 to 2.

The correlations of the measurements were also analyzed (Table 4). While the variations of the LA diameters were moderately correlated with UH from stage 0 to 2, the correlation coefficient with midvagina was weak; nevertheless, distal vagina and mid-LA showed no correlation. Then from stage 2 to 3, there were relationships between each other among apex vagina, midvagina, distal vagina, LA diameters, and UH.

The correlations between degree of prolapse and LPA, ARA, length of PVW, and PD were 0.405 ($P < 0.001$), 0.352 ($P < 0.01$), 0.419 ($P < 0.001$), and 0.572 ($P < 0.001$), respectively, but there was no correlation with straight-line distance of PVW.

DISCUSSION

To our knowledge, we first presented a possible mechanism of PVP based on the quantified displacements from the perspective of mechanical equilibrium and described a detailed procedure for how the pressure and supporting force interaction contributes to the formation of the PVW and the supporting structures in the progressive degrees of PVP. To better demonstrate and comprehend the hypothesis, the continuous progress was segmented artificially and described as follows.

Here, a basic structural paradigm[12] was needed to help guide discussion: the uterosacral-cardinal ligament and the uterus are compared with "slack cord" and "boat," respectively; uterus position is not decided by the ligaments tethering the boat to the dock primarily, but by the surrounding structures such as "water." Linear relationship between pressure and displacement[13] could also help to illuminate the hypothesis.

From stage 0 to 2, because of the curving model[14,15] and physiologic elastic range,[16] the pull of uterosacral-cardinal ligament was considered zero, despite the incremental displacement of apex vagina.[12] Thus, the pressure difference directly exerted on LA and the diameters of LA increased. When the LA appeared to block

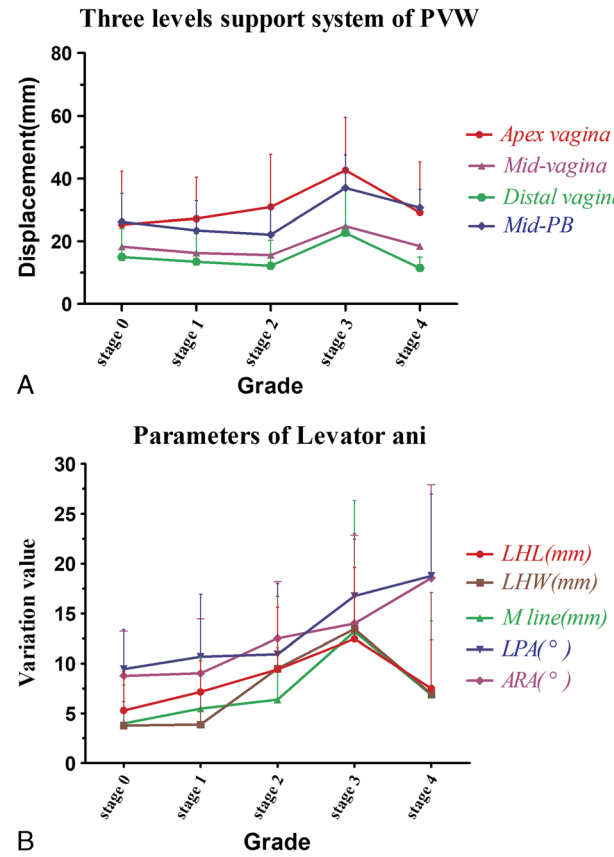

FIGURE 2. Variation in structural support parameters from rest to maximum Valsalva with normal women and increasing degrees of PVP. A, Magnitude (in mm) of displacement in 3 levels of the vaginal support system of the PVW (level I: apex vagina; level II: midvagina; level III: distal vagina, mid-PB). B, Variation of the LA (distance [in mm]: LHL, LHW, ML; angle [°]: LPA, ARA).

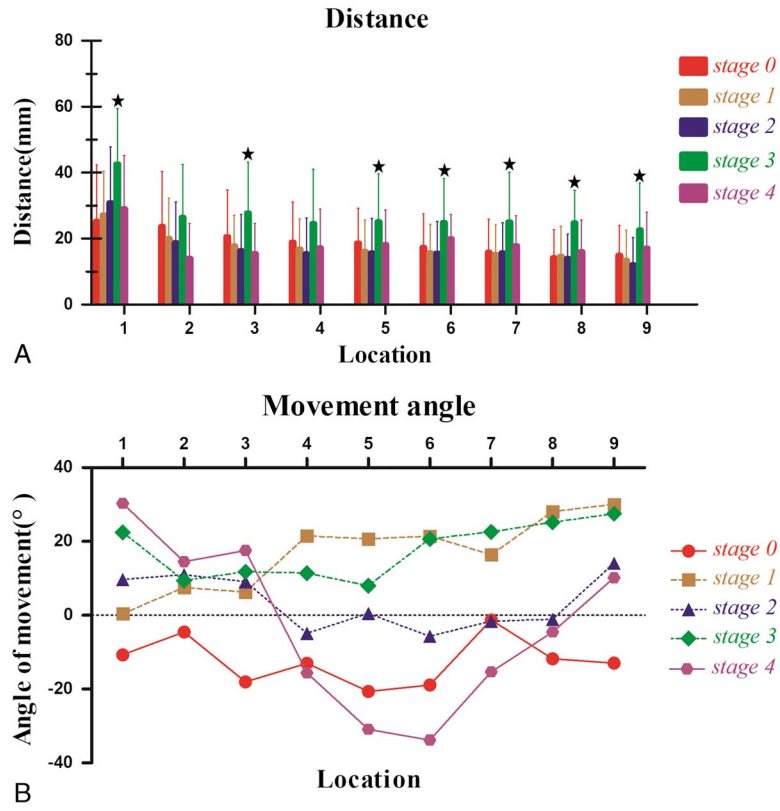

FIGURE 3. A, Mean magnitude (in mm) of displacement measured at 9 locations along the PVW. Error bars represent SEs, whereas asterisks (*) indicate statistically significant differences of the locations at which displacement occurs ($P < 0.05$). B, Angle of displacement (degrees from the vertical) in normal women and women with different degrees of PVP.

most of the pressure, the rest applied to levels II and III supports became smaller; thus, the displacement of midvagina, distal vaginal, and mid-PB became less, and the deformation of the lower two-thirds of PVW was not obvious. Besides, the displacement of mid-PB was greater than that of midvagina and distal vagina, which means PB gets more stress compared with two others. Jing et al[17] also reported that the muscle near the PB region takes the greatest strain.

From stage 2 to 3, the impairment of pelvic floor continued to increase, the resistance of LA was no longer sufficient, and so the vaginal support structure appeared to initiate a suspending and sustaining function. At this moment, although the "slack"

TABLE 3. Movement Angle (°) (Degrees From the Vertical) in Normal Women and Women With Different Stages of PVP

Point	Stage 0 (n = 12)	Stage 1 (n = 18)	Stage 2 (n = 24)	Stage 3 (n = 11)	Stage 4 (n = 9)	ANOVA *P*
1	−10.7 ± 14.1	0.4 ± 9.1	9.7 ± 8.9	22.5 ± 9.8	30.3 ± 7.9	0.124
2	−4.5 ± 15.8	7.5 ± 9.7	11.0 ± 8.6	9.4 ± 10.5	14.5 ± 9.3	0.840
3	−18.0 ± 12.7	6.3 ± 9.3	9.1 ± 9.2	11.8 ± 10.3	17.6 ± 12.7	0.290
4	−13.0 ± 13.5	21.5 ± 7.5	−4.9 ± 8.4	11.4 ± 11.0	−15.6 ± 11.7	0.058
5	−20.6 ± 12.4*	20.7 ± 6.4†	0.5 ± 6.6‡	8.0 ± 9.3*§	−30.9 ± 10.4†‡§	0.001
6	−18.9 ± 10.6	21.4 ± 5.4†	−5.7 ± 6.8‡‖	20.7 ± 9.3§‖	−33.8 ± 7.5†‡§	0.000
7	−1.3 ± 13.9	16.4 ± 6.1†	−1.6 ± 8.6‡‖	22.6 ± 9.6§‖	−15.3 ± 6.8†‡§	0.047
8	−11.8 ± 10.2*	28.1 ± 5.3†	−1.1 ± 7.1‖	25.2 ± 8.7§*‖	−4.5 ± 7.4†§	0.001
9	−12.9 ± 17.4	30.0 ± 9.7	14.1 ± 10.4	27.5 ± 11.2	10.2 ± 10.6	0.147

Values are reported as mean ± SD. *P* values were determined using ANOVA for comparisons of means and least significance difference test for parity. Movement angle is the angle between the direction of movement and the long axis of the body. Positive to the dorsal, negative to the ventral.

*Pairwise: stage 3 versus stage 0 ($P < 0.05$).

†Pairwise: stage 4 versus stage 1 ($P < 0.001$).

‡Pairwise: stage 4 versus stage 2 ($P < 0.01$).

§Pairwise: stage 4 versus stage 3 ($P < 0.05$).

‖Pairwise: stage 3 versus stage 2 ($P < 0.05$).

TABLE 4. . Correlation Coefficients Between Different Levels of Vaginal Support, LA, and UH

		Apex Vagina		Midvagina		Distal Vagina		UH	
	Stage	*r*	*P*	*r*	*P*	*r*	*P*	*r*	*P*
LHL	0–2	—	—	0.309	0.023	0.125	0.368	0.469	0.000
	2–3	0.619	0.000	0.639	0.000	0.368	0.030	0.567	0.000
LHW	0–2	—	—	0.219	0.111	−0.065	0.638	0.317	0.02
	2–3	0.678	0.000	0.582	0.000	0.270	0.117	0.441	0.008
ML	0–2	—	—	0.431	0.001	0.184	0.182	0.515	0.000
	2–3	0.527	0.001	0.639	0.000	0.519	0.001	0.516	0.001
LPA	0–2	—	—	0.295	0.030	0.232	0.091	0.298	0.029
	2–3	0.313	0.068	0.485	0.003	0.349	0.040	0.523	0.001
Midvagina	2–3	0.831	0.000	—	—	0.586	0.000	0.784	0.000
Distal vagina	2–3	0.394	0.019	0.586	0.000	—	—	0.352	0.038
UH	2–3	0.708	0.000	0.784	0.000	0.352	0.038	—	—
Mid-LA	2–3	0.120	0.491	0.207	0.232	0.479	0.004	0.229	0.186

LHL indicates length of LA; LHW, width of LA; midvagina, mean displacement of points 4 to 6.

cord transformed into "tighten"[15] and started to resist pressure, it was still inadequate for contending against the growing pressure difference. The remaining pressure passed down to levels II and III support; thus, displacement of vaginal supports and LA diameters ascended and peaked at stage 3 with the similar movement circle. The vaginal wall also participated in maintaining resistance by enlarging effective stress area and altering shape, and length of PVW was related to degree of prolapse moderately. When vaginal support resisted powerless, PVW deformed violently, the entire PVW shifted downward, and the movement angle for the upper and lower portions were posterior toward the rectum and slightly caudal, whereas the middle portion moved ventral, and finally protrusion emerged. These findings of the deformation path of PVW were in agreement with a previous report by Lewicky-Gaupp et al.[7]

In the current phase, we found that correlation coefficient of level I versus lower elements (levels II and III and UH) was larger than LA versus lower elements at stage 0 to 2 universally. In addition, the displacement vector of apex vagina exceeded others; thus, apical support withstood the largest portion of loads and was the one closest to PVP. Haylen et al[18] also reported midvagina slack was caused by the descent of the apex vagina, and Rooney et al[19] found a significant correlation between apex vagina and the posterior prolapse. Furthermore, the rising slope of mid-PB displacement overtaking apex vagina and midvagina could mean the role of level III support was enhanced.

From stage 3 to 4, the vagina support system deteriorated; the PVW could barely return to normal anatomical position in resting state, so the displacement of measurements started to decline. The increasing angle of LPA and ARA also indicated the growing impairment of LA.[20] We also found movement angle of the lower segment of PVW was significantly different between stage 3 to 4 and stage 0 to 2; it could be the bulging vagina wall outside uncontrolled introitus. Bulging became the way to achieve balance on another level, which could be explained by the displacement of apex vagina being close to mid-PB, looking similar to that at stage 0.

Nevertheless, the hypothesis generating insight into the potential mechanisms of PVP seemed to exaggerate the dynamic MRI data only; thus, some limitations should be considered when interpreting the data. First, we need to understand the actual mechanical distribution should be much more complex on the natural stereoscopic 3D rather than on a 2-dimensional plane. Second, we also need to understand that other pathogenesis contributed to PVP despite that the mechanical mechanism was the focus in this study. Third, the cross-sectional results represented only some point in the process of prolapse that occurs or progresses linearly.

The present study showed possible mechanical mechanisms of PVP in detail. However, as yet, there is no convincing evidence that can verify the hypothesis. Future studies should address measuring the actual mechanical stress incurred by different locations in vivo in real time, for instance, an innovative equipment or a revolutionary method, which is likely to provide insight into the mechanisms underlying the interaction of supporting structures.

In summary, quantified displacements on MRI could be used to hypothesize the mechanical mechanisms of PVP regarding the interaction between pressure and the support force contributing to the deformation of PVW and the supporting structures.

REFERENCES

1. Boyles SH, Weber AM, Meyn L. Procedures for pelvic organ prolapse in the United States, 1979–1997. *Am J Obstet Gynecol* 2003; 188(1):108–115.
2. Silva WA, Pauls RN, Segal JL, et al. Uterosacral ligament vault suspension: five-year outcomes. *Obstet Gynecol* 2006;108(2):255–263.
3. Olsen AL, Smith VJ, Bergstrom JO, et al. Epidemiology of surgically managed pelvic organ prolapse and urinary incontinence. *Obstet Gynecol* 1997;89(4):501–506.
4. Fialkow MF, Newton KM, Lentz GM, et al. Lifetime risk of surgical management for pelvic organ prolapse or urinary incontinence. *Int Urogynecol J Pelvic Floor Dysfunct* 2008;19(3):437–440.
5. Soligo M. Posterior pelvic floor dysfunction: there is an immediate need to standardize terminology. *Int Urogynecol J Pelvic Floor Dysfunct* 2007; 18(4):369–371.
6. Kelvin FM, Maglinte DD, Hornback JA, et al. Pelvic prolapse: assessment with evacuation proctography (defecography). *Radiol* 1992;184(2): 547–551.
7. Lewicky-Gaupp C, Yousuf A, Larson KA, et al. Structural position of the posterior vagina and pelvic floor in women with and without posterior vaginal prolapse. *Am J Obstet Gynecol* 2010;202(5):1–6.
8. Spahlinger DM, Newcomb L, Ashton-Miller JA, et al. Relationship between intra-abdominal pressure and vaginal wall movements during Valsalva in women with and without pelvic organ prolapse: technique development and early observations. *Int Urogynecol J* 2014;25(7): 873–881.

9. Summers A, Winkel LA, Hussain HK, et al. The relationship between anterior and apical compartment support. *Am J Obstet Gynecol* 2006; 194(5):1438–1443.
10. Hsu Y, Summers A, Hussain HK, et al. Levator plate angle in women with pelvic organ prolapse compared to women with normal support using dynamic MR imaging. *Am J Obstet Gynecol* 2006;194(5): 1427–1433.
11. Delancey JO. Anatomie aspects of vaginal eversion after hysterectomy. *Am J Obstet Gynecol* 1992;166(6 pt 1):1717–1728.
12. Smith TM, Luo J, Hsu Y, et al. A novel technique to measure in vivo uterine suspensory ligament stiffness. *Am J Obstet Gynecol* 2013;209(5):484 e481–484 e487.
13. Yun P, Khavari R, Nakib NA, et al. Assessment of urethral support using MRI-derived computational modeling of the female pelvis. *Int Urogynecol J* 2015;27(2):205–212.
14. Chen L, Ramanah R, Hsu Y, et al. Cardinal and deep uterosacral ligament lines of action: MRI based 3D technique development and preliminary findings in normal women. *Int Urogynecol J* 2013;24(1): 37–45.
15. Ramanah R, Berger MB, Chen L, et al. See it in 3D!: researchers examined structural links between the cardinal and uterosacral ligaments. *Am J Obstet Gynecol* 2012;207(5):1–7.
16. Rahn DD, Ruff MD, Brown SA, et al. Biomechanical properties of the vaginal wall: effect of pregnancy, elastic fiber deficiency, and pelvic organ prolapse. *Am J Obstet Gynecol* 2008;198(5):590–e591.
17. Jing D, Ashton-Miller JA, DeLancey JO. A subject-specific anisotropic visco-hyperelastic finite element model of female pelvic floor stress and strain during the second stage of labor. *J Biomech* 2012; 45(3):455–460.
18. Haylen BT, Naidoo S, Kerr SJ, et al. Posterior vaginal compartment repairs: where are the main anatomical defects? *Int Urogynecol J* 2016; 27(5):741–745.
19. Rooney K, Kenton K, Mueller ER, et al. Advanced anterior vaginal wall prolapse is highly correlated with apical prolapsed. Am J Obstet Gynecol 2016;195(6):1837–1840.
20. Rostaminia G, White DE, Quiroz LH, et al. Levator plate descent correlates with levator ani muscle deficiency. *Neurourol Urodynamics* 2013; 34(1):55–59.